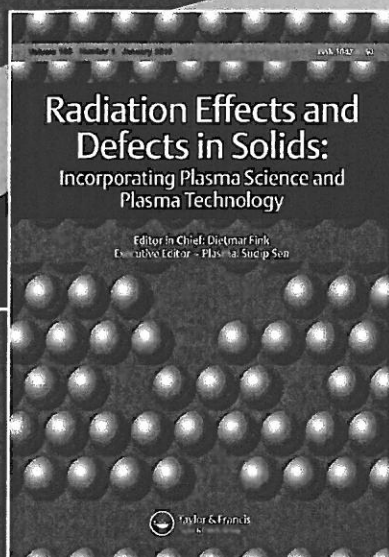


Call for Special Issue Papers: Space, Fusion and Technological Plasmas



Radiation Effects and Defects in Solids: Incorporating Plasma Science and Plasma Technology

Editor:

D. Fink

Universidad Autónoma,
Metropolitana-Iztapalapa

Executive Editor - Plasma:

S. Sen

National Institute of Aerospace,
College of William & Mary,
Lancaster University

Guest Editors:

George V. Khazanov

Professor and Senior Scientist,
NASA-Goddard, Greenbelt, Maryland,
USA (Space Plasma)

Wayne A. Scales

Professor and Director, Center of Space
Science and Engineering Research,
Virginia Tech, Blacksburg, Virginia, USA
(Space Plasma)

George Vahala

Professor, College of William and Mary,
Williamsburg, Virginia, USA
(Fusion Plasma)

Chijin Xiao

Professor, University of Saskatchewan,
Saskatoon, Canada
(Technological Plasma)

In this special plasma issue of REDS papers are solicited on space, fusion and technological plasmas - all aspects of theoretical, numerical and experimental investigations and review articles are solicited. The standard page limits for the journal will be followed with some exceptions to the review papers.

Submission Guidelines

All papers for consideration should be submitted online at the ***Radiation Effects and Defects in Solids*** ScholarOne ManuscriptsTM site at: <http://mc.manuscriptcentral.com/grad>

Please include on the title page that the paper is intended for the special issue on: "Space, Fusion and Technological Plasmas."

For further information, visit the journal's homepage and click on 'Authors and submissions / Instructions for authors'

**Submission deadline:
31st March 2013**

www.tandfonline.com/grad



Taylor & Francis
Taylor & Francis Group

Call for Special Issue Papers: Space, Fusion and Technological Plasmas

Why submit your article to **Radiation Effects and Defects in Solids?**

Wide dissemination

Through excellent international reach, publishing in *Radiation Effects and Defects in Solids* ensures that your article is seen, read and cited by your research community.

Fast and professional peer review

All research articles in *Radiation Effects and Defects in Solids* undergo a stringent peer review process, based on initial editor screening and anonymized refereeing by at least two undisclosed referees.

Author support from Taylor & Francis

The author services department at Taylor & Francis aims to enhance your publishing experience and to optimise the impact of your article in the global research community. Support is available, from preparing and submitting your article, through to setting up citation alerts post-publication.

For further details visit <http://journalauthors.tandf.co.uk/>

Visit the journal homepage to:

- Submit your research
- Register for table of contents alerts
- Discover most read & most cited articles
- Access the latest journal's news & offers
- View the full Editorial Board

Don't miss out!

Register to receive table of
contents alerts for
Radiation Effects and Defects in Solids.

Click on 'Alert me' below the cover
on the journal's homesite.



substrates^{22,23}, although there are still some remaining challenges with this step. Finally, processes have been developed to fabricate devices with this single atomic layer material²⁴.

The operational principle of most of the graphene sensors demonstrated so far is very similar to that of solid state sensors. As gas molecules adsorb onto graphene's surface, they act as either electron donors or acceptors, inducing a local change in the electrical conductivity in graphene^{1,9}. This effect is very pronounced in graphene due to the combination of some excellent properties, namely, high surface area, high electrical conductivity, and inherently low noise, making it possible to detect the smallest of changes in resistance. Atomic oxygen, on the other hand, can react with carbon atoms of graphene to form epoxide and carboxylic groups, and change the sp^2 hybridization into sp^3 in the process, giving rise to the possibility of even greater sensitivity. The conductivity of graphene has been demonstrated to decrease significantly, up to a few orders of magnitude, as graphene oxidizes, with the conductivity as well as optical transparency depending strongly on the level of oxidation²⁵. Furthermore, single layer graphene has been shown to be more reactive with oxygen species, thus increasing the sensitivity further, than multilayer graphene²⁶.

Atomic oxygen (AO) usually forms in the thermosphere when molecular oxygen dissociates upon exposure to solar ultraviolet radiation. Since the vertical density distributions of gases in the ionosphere are determined by the free molecular flow, they usually stratify according to their molecular mass and AO predominates in the altitude range of 200-650 km²⁷. The AO density distribution varies widely with the level of solar irradiation, and thus the latitude, longitude, local time, season and the solar cycle. Thermospheric models can somewhat predict the AO concentrations and fluxes; however, such predictions often have as large an error as 25% or higher²⁷. Improved data on the AO concentrations and fluxes can have significant impact not only in the understanding of the physics and chemistry of the upper atmosphere, but also in the design of commercial, military, and scientific spacecrafts. This article discusses how the novel graphene chemical sensors can be used for in situ measurements of AO concentration and the impact this technology may have on a number of heliophysics and space applications.

Experimental Details

Large area graphene was synthesized on 3"x3" Copper foils (25 um thick) by Low Pressure Chemical Vapor Deposition (LPCVD). Copper foils were pretreated in dilute nitric acid and flatly placed in a 3" diameter tube. Growth was carried out at 1000°C and 1Torr for 40 minutes under the flow of hydrogen and argon with methane as the carbon source. After growth was complete, the tube was quickly cooled down by flowing cold nitrogen gas at the center of the tube and flowing air at the two ends of the tube. 2"x1" graphene-on-copper pieces were cut out and were transferred onto silicon wafers with a 300 nm of thermally grown oxide film. A 250-nm thick poly(methylmethacrylate) (PMMA) layer was spun on graphene on the frontside of the copper foil and graphene on the backside of the foil was removed with oxygen plasma. The exposed side of the

copper foil was then floated on iron chloride solution in order to etch copper. After that, PMMA coated graphene was rinsed in deionized water a few times, followed by a rinse in 10% hydrochloric acid to remove any adsorbed ions of iron chloride. After properly rinsing the film in deionized water a second time, graphene was transferred onto a silicon substrate and PMMA was removed by annealing in the vacuum oven at 350°C for 2 hours while flowing hydrogen and argon.

Raman mapping was performed to characterize the quality and the number of layers of the synthesized graphene. An automated confocal Raman Microscope (Horiba Yvon LabRam ARAMIS) was used with a 532 nm laser and a swift detector. The spot size of the system was 400 nm.

Arrays of graphene sensors were fabricated on silicon wafers with a 300-nm thermal oxide layer by photolithography. First, a 4-nm titanium and 20-nm gold layer were deposited as the contacts with e-beam evaporation using a lift-off process. Next, graphene is transferred on the wafer as described above and a thin PMMA layer was spun to protect graphene from any contamination due to resist or solvents. Next, a positive photoresist (Shipley 1827) was used to pattern graphene and oxygen plasma was used to etch through both PMMA and graphene. Finally, a thick layer of gold was deposited for the contact pads with e-beam evaporation using a shadow mask. The gold pads were finally wirebonded to a homemade chip carrier on pyrex wafers.

Results and Discussion

Microscopy and spectroscopy data demonstrated that the synthesized large area graphene is of high quality and with low defect density. Figure 1 a presents an optical microscopy image of a 2"x1" graphene piece transferred to a silicon substrate. Figure 1 b shows the Raman spectrum of a random spot on the sample. The number of layers in a graphene sample can be determined from the intensity of its characteristic peaks: G and 2D peak. Also, the quality of synthesized graphene can be quantified with the D peak, representing the defect density. The ratio of the 2-D peak intensity and the G peak intensity of graphene synthesized in our lab was greater than 3, and the Full Width at Half Maximum (FWHM) of the 2-D peak was in the range of 35 and 40. Both of these features are characteristic of single layer graphene²⁸. In addition, the low intensity of the D peak implies minimal defect density. Figure 1 c presents Raman mapping data over a 20µm x 20µm area of the graphene sample. It plots the intensity ratio of the two characteristic peaks of graphene, namely 2-D and G peak, as a function of the x- and y-coordinate. The plot shows that the intensity ratio is quite uniform over tens of microns and the entire area is mostly single layer.

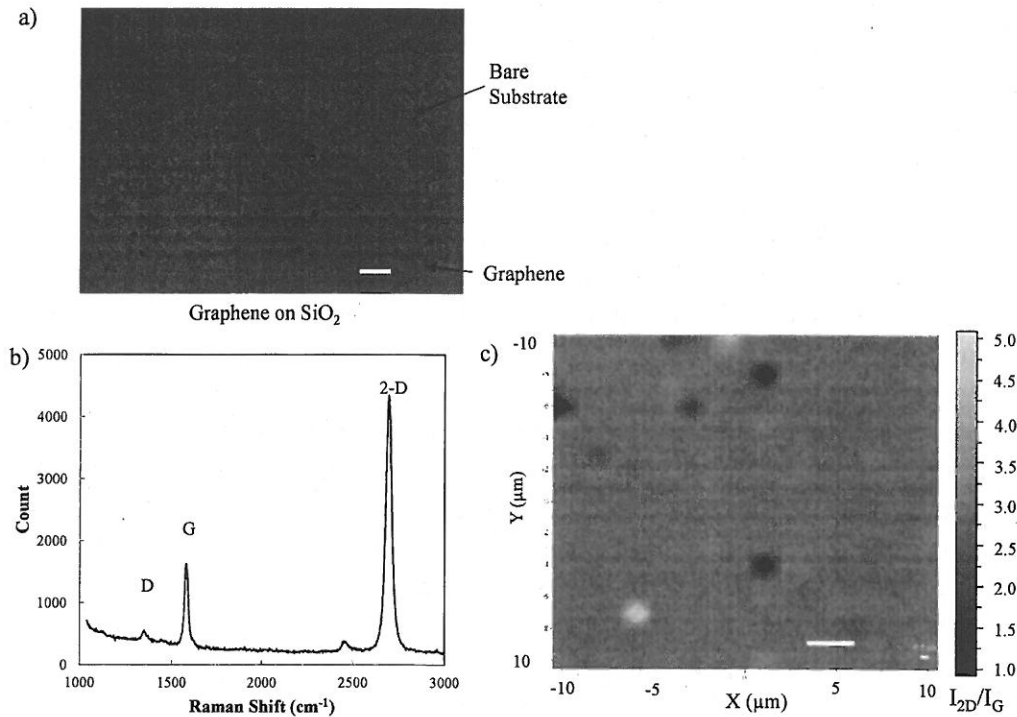


Figure 1. a) Optical microscopy image of large area graphene on a silicon dioxide substrate (5 micron bar); b) Single spot Raman Spectrum of the synthesized graphene demonstrating single layer and low defects. C) Intensity ratio of 2-D and G peak of a Raman map over a 20µm x 20µm area demonstrating the uniformity of single layer coverage (2.5 micron bar).

Sensors with varied widths and lengths of graphene ranging from 5µm to 500 µm were designed. Each chip was configured to test multiple sensors simultaneously. Commercial temperature sensors were bonded on the chip and were hooked up to a temperature controller from Lakeshore. Figure 2a shows a typical chip layout. A homebuilt test setup is currently being used for characterizing the sensor array with test gases. The test setup includes a vacuum chamber connected to a Turbo pump, a computerized multi-component gas mixing and dilution system from Environics Inc. to deliver commercial gases, a Keithley Source Measure Unit (2400) for data collection and a Keithley Multiplexing Unit for simultaneous measurements of multiple sensing elements. Figure 2b presents a schematic of the test setup. On-chip heaters are used to desorb any species or contaminants from the chips and heating tapes are used to outgas the chamber before performing any tests.

We are currently incorporating an atomic oxygen beam with our test setup in order to characterize device performance in the presence of atomic oxygen. The potential atomic oxygen detector could be used in series with Stark effect to make a powerful tool to separate and detect species.

Graphene sensors can be used to measure the concentration of atomic oxygen, as well as other neutral species, without having to ionize them. This capability can have large impact on a variety of space applications. Firstly, the ability to determine neutral

densities can prove an avenue to significantly resolve the density measurement uncertainty, which in turn can improve the density models used by NASA and DOD.

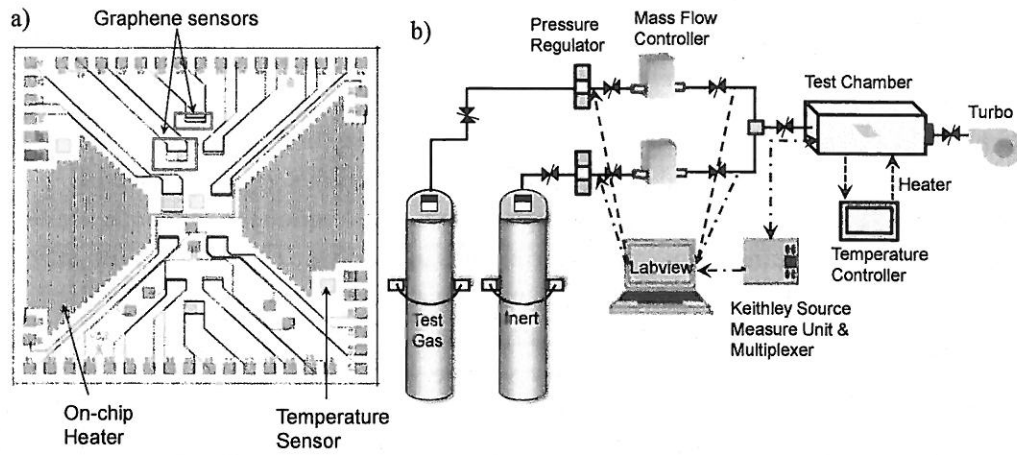


Figure 2. a) Chemical sensor chip with an array of ten sensing elements; b) Schematic of the test setup.

Improved models can more accurately predict the damage and erosion of spacecrafts due to atomic oxygen, and assist in better designs for the spacecrafts. An array of graphene sensors can be used in neutral atom imaging missions such as Low Energy Neutral Atom (LENA).

Spatiotemporally resolved concentrations of AO can be obtained with in situ measurements enabled by the sensitive graphene sensor arrays. Such measurements in the upper atmosphere at 400 km altitude can provide a description of the motion of the thermosphere and ionosphere due to extreme ultraviolet radiation as never before. Similarly, in situ measurements of AO in the auroral regions will potentially be able to continuously monitor the state of neutral atmosphere, as well as its response in time and space during auroral heating events.

In addition, highly sensitive graphene sensors can provide a potential solution to a crucial Space Weather problem: the prediction of duration and location of Geomagnetically Induced Currents (GICs). The developed sensor arrays promise to provide instantaneous monitoring of the state of the upper atmosphere with sufficient detail for GIC prediction.

Furthermore, a network of graphene chemical sensors will be suitable for a wide range of mission architectures in Planetary Sciences, both atmospheric probes and landed missions. The Planetary Science Decadal Survey names Titan/Saturn System Mission, Neptune Orbiter and Probe, and Mars Sample Return as high priority missions²⁹; the versatility of graphene sensors with respect to operating conditions and ability to customize and select gases of interest makes them competitive for a broad range of missions. Graphene sensors can detect gases that can help fingerprint various biological and geochemical processes on other planetary bodies such as outer planets, moons and asteroids. A network of these cheap, tiny sensors deployed on the surface of

a planetary body can make simultaneous measurements in many locations, which can be used to construct a map of surface composition. This is in contrast to the current scenario where measurements are performed at one location at a time, and hence only a limited number of measurements can be made over the lifetime of the mission.

Conclusion

Graphene chemical sensors have been explored for a variety of applications in the recent past, including homeland security, monitoring hazardous gases in chemical industry and labs for safety, and monitoring environmental pollutants for public health. However, one of the most significant contributions of graphene chemical sensors may be in space science. In fact, these compact and miniaturized sensor platforms can realize the concept of Femto-Sats, which can potentially enable many new science missions in Heliophysics, Earth Science, and Planetary Science. The ability of these low mass, low power sensors to detect neutral species without having to ionize them makes them extremely attractive for many space applications, including atmospheric probes for planetary bodies; neutral atom imaging missions; resolving the density measurement uncertainty in the ionosphere through the measurement of atomic oxygen concentration; imaging the motion of thermosphere and ionosphere; and predicting geomagnetically induced currents.

References

- 1 Schedin, F. *et al.* Detection of individual gas molecules adsorbed on graphene. *Nat. Mater.* **6**, 652-655, doi:10.1038/nmat1967 (2007).
- 2 Geim, A. K. & Novoselov, K. S. The rise of graphene. *Nat. Mater.* **6**, 183-191, doi:10.1038/nmat1849 (2007).
- 3 Novoselov, K. S. *et al.* Two-dimensional gas of massless Dirac fermions in graphene. *Nature* **438**, 197-200, doi:10.1038/nature04233 (2005).
- 4 Novoselov, K. S. *et al.* A roadmap for graphene. *Nature* **490**, 192-200, doi:10.1038/nature11458 (2012).
- 5 Bolotin, K. I., Sikes, K. J., Hone, J., Stormer, H. L. & Kim, P. Temperature-dependent transport in suspended graphene. *Phys. Rev. Lett.* **101**, doi:10.1103/PhysRevLett.101.096802 (2008).
- 6 Lee, C., Wei, X. D., Kysar, J. W. & Hone, J. Measurement of the elastic properties and intrinsic strength of monolayer graphene. *Science* **321**, 385-388, doi:10.1126/science.1157996 (2008).
- 7 Bunch, J. S. *et al.* Impermeable atomic membranes from graphene sheets. *Nano Lett.* **8**, 2458-2462, doi:10.1021/nl801457b (2008).
- 8 Perkins, F. K. *et al.* Chemical Vapor Sensing with Mono layer MoS₂. *Nano Lett.* **13**, 668-673, doi:10.1021/nl3043079 (2013).
- 9 Dan, Y. P., Lu, Y., Kybert, N. J., Luo, Z. T. & Johnson, A. T. C. Intrinsic Response of Graphene Vapor Sensors. *Nano Lett.* **9**, 1472-1475, doi:10.1021/nl8033637 (2009).
- 10 Fowler, J. D. *et al.* Practical Chemical Sensors from Chemically Derived Graphene. *ACS Nano* **3**, 301-306, doi:10.1021/nn800593m (2009).
- 11 Lu, G. H. *et al.* Toward Practical Gas Sensing with Highly Reduced Graphene Oxide: A New Signal Processing Method To Circumvent Run-to-Run and

- Device-to-Device Variations. *ACS Nano* **5**, 1154-1164, doi:10.1021/nn102803q (2011).
- 12 Robinson, J. T., Perkins, F. K., Snow, E. S., Wei, Z. Q. & Sheehan, P. E. Reduced Graphene Oxide Molecular Sensors. *Nano Lett.* **8**, 3137-3140, doi:10.1021/nl8013007 (2008).
- 13 Wu, W. *et al.* Wafer-scale synthesis of graphene by chemical vapor deposition and its application in hydrogen sensing. *Sens. Actuator B-Chem.* **150**, 296-300, doi:10.1016/j.snb.2010.06.070 (2010).
- 14 Yavari, F. *et al.* High Sensitivity Gas Detection Using a Macroscopic Three-Dimensional Graphene Foam Network. *Sci Rep* **1**, doi:10.1038/srep00166 (2011).
- 15 Yuan, W. J., Liu, A. R., Huang, L., Li, C. & Shi, G. Q. High-Performance NO₂ Sensors Based on Chemically Modified Graphene. *Adv. Mater.* **25**, 766-771, doi:10.1002/adma.201203172 (2013).
- 16 Huang, J., Zhang, L., Liang, R. P. & Qiu, J. D. "On-off" switchable electrochemical affinity nanobiosensor based on graphene oxide for ultrasensitive glucose sensing. *Biosens. Bioelectron.* **41**, 430-435, doi:10.1016/j.bios.2012.09.007 (2013).
- 17 Wang, Q. & Yun, Y. B. Nonenzymatic sensor for hydrogen peroxide based on the electrodeposition of silver nanoparticles on poly(ionic liquid)-stabilized graphene sheets. *Microchim. Acta* **180**, 261-268, doi:10.1007/s00604-012-0921-3 (2013).
- 18 Emtsev, K. V. *et al.* Towards wafer-size graphene layers by atmospheric pressure graphitization of silicon carbide. *Nat. Mater.* **8**, 203-207, doi:10.1038/nmat2382 (2009).
- 19 Li, X. S. *et al.* Large-Area Synthesis of High-Quality and Uniform Graphene Films on Copper Foils. *Science* **324**, 1312-1314, doi:10.1126/science.1171245 (2009).
- 20 Reina, A. *et al.* Large Area, Few-Layer Graphene Films on Arbitrary Substrates by Chemical Vapor Deposition. *Nano Lett.* **9**, 30-35, doi:10.1021/nl801827v (2009).
- 21 Park, S. & Ruoff, R. S. Chemical methods for the production of graphenes. *Nat. Nanotechnol.* **4**, 217-224, doi:10.1038/nnano.2009.58 (2009).
- 22 Li, X. S. *et al.* Transfer of Large-Area Graphene Films for High-Performance Transparent Conductive Electrodes. *Nano Lett.* **9**, 4359-4363, doi:10.1021/nl902623y (2009).
- 23 Kobayashi, T. *et al.* Production of a 100-m-long high-quality graphene transparent conductive film by roll-to-roll chemical vapor deposition and transfer process. *Appl. Phys. Lett.* **102**, doi:10.1063/1.4776707 (2013).
- 24 Hsu, A., Wang, H., Kim, K. K., Kong, J. & Palacios, T. Impact of Graphene Interface Quality on Contact Resistance and RF Device Performance. *IEEE Electron Device Lett.* **32**, 1008-1010, doi:10.1109/led.2011.2155024 (2011).
- 25 Jung, I., Dikin, D. A., Piner, R. D. & Ruoff, R. S. Tunable Electrical Conductivity of Individual Graphene Oxide Sheets Reduced at "Low" Temperatures. *Nano Lett.* **8**, 4283-4287, doi:10.1021/nl8019938 (2008).
- 26 Liu, L. *et al.* Graphene oxidation: Thickness-dependent etching and strong chemical doping. *Nano Lett.* **8**, 1965-1970, doi:10.1021/nl0808684 (2008).
- 27 Osborne, J. J., Harris, I. L., Roberts, G. T. & Chambers, A. R. Satellite and rocket-borne atomic oxygen sensor techniques. *Rev. Sci. Instrum.* **72**, 4025-4041, doi:10.1063/1.1406928 (2001).

- 28 Ferrari, A. C. *et al.* Raman spectrum of graphene and graphene layers. *Phys. Rev. Lett.* **97**, doi:10.1103/PhysRevLett.97.187401 (2006).
- 29 The Planetary Decadal Survey for 2013-2022. (2011).